Analytica Chimica Acta xxx (2018) 1–11

Contents lists available at ScienceDirect

Analytica Chimica Acta

journal homepage: www.elsevier.com/locate/aca

Red emission nitrogen, boron, sulfur co-doped carbon dots for "on-off-on" fluorescent mode detection of Ag^+ ions and L-cysteine in complex biological fluids and living cells

Shan Huang [a, b], Erli Yang [a], Jiandong Yao [a], Yi Liu [a, b], Qi Xiao [a, b, *]

[a] College of Chemistry and Materials Science, Guangxi Key Laboratory of Natural Polymer Chemistry and Physics, Guangxi Teachers Education University, Nanning 530001, PR China
[b] College of Chemistry and Molecular Sciences, Wuhan University, Wuhan 430072, PR China

HIGHLIGHTS

- One-step hydrothermal synthesis of red emission NBS-CDs is reported.
- NBS-CDs exhibit excellent biocompatibility and negligible cytotoxicity to human cancer cells.
- NBS-CDs-based fluorescent "on-off-on" sensor was applied for Ag^+ and L-Cys determination.
- This fluorescent "on-off-on" sensor was used for visual detection of Ag^+ and L-Cys in living cells.

GRAPHICAL ABSTRACT

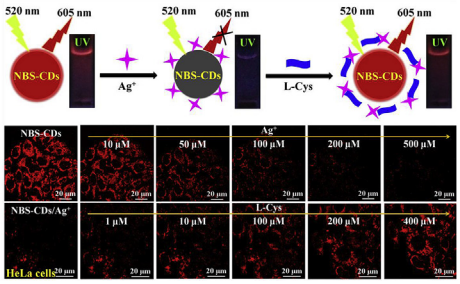

ARTICLE INFO

Article history:
Received 23 March 2018
Received in revised form
21 May 2018
Accepted 14 June 2018
Available online xxx

Keywords:
Red emission carbon dots
Ag(I) ion
L-cysteine
Determination
Living cells imaging

ABSTRACT

Herein, a simple and efficient fluorescent assay for Ag^+ ions and L-cysteine (L-Cys) in complex biological fluids and living cells was first developed based on the fluorescent "on-off-on" mode of red emission nitrogen, boron, sulfur co-doped carbon dots (NBS-CDs). Red emission NBS-CDs were prepared via one-step hydrothermal synthesis by using 3-aminobenzeneboronic acid and 2,5-diaminobenzenesulfonic acid as precursors. Such NBS-CDs exhibited excellent optical properties and relatively high absolute fluorescent quantum yield compared with some reported NBS-CDs. Due to the strong quenching ability of Ag^+ ions on the fluorescence of NBS-CDs, red emission NBS-CDs were used for the determination of Ag^+ ions with high sensitivity and excellent selectivity. The fluorescence of NBS-CDs was recovered after the interaction between Ag^+ ions and L-Cys, which realized the specific determination of L-Cys in human urine samples and human plasma samples. The established NBS-CDs-based fluorescent "on-off-on" sensor offered a relatively low detection limits of 0.35 μM for Ag^+ ions and 0.045 μM for L-Cys based on three times signal-to-noise criteria. Notably, this strategy was applied for the visual detections of Ag^+ ions and L-Cys in living human cancer cells (HeLa cells and MCF-7 cells). This method is simple, high sensitive, and excellent selectivity, which provided a new insight on the potential applications of NBS-CDs to develop the biosensor in clinical diagnosis and other biologically related areas.

1. Introduction

As a fascinating type of "zero-dimensional" carbon-based

* Corresponding author. College of Chemistry and Materials Science, Guangxi Key Laboratory of Natural Polymer Chemistry and Physics, Guangxi Teachers Education University, Nanning 530001, PR China.
E-mail address: qi.xiao@whu.edu.cn (Q. Xiao).

https://doi.org/10.1016/j.aca.2018.06.051
0003-2670/

nanomaterials, carbon dots (CDs) have drawn huge attentions in diverse areas due to their easy preparation, unique optical, electronic, and biocompatible properties [1–3]. In recent years, doped CDs are recognized as an emerging field of carbon-based nanomaterials, since heteroatoms doping can efficiently tailor the surface defects, tune the electronic energy levels, and modify the optical properties of CDs [4,5]. Nitrogen (N), sulfur (S), and boron (B), which are the neighboring atoms with similar atomic radii of carbon in the periodic table, are the most popular doping atoms in CDs to efficiently promote their fluorescence properties and provide available functional groups for target sensing [6–10]. Cheng et al. reported the synthesis of B, S, and N co-doped CDs as fluorescent probe for selective and sensitive detection of sunset yellow [7]. Especially, red emission CDs with doping of some special heteroatoms exhibit great potential applications in important bio-related regions. Sun et al. developed a facile route to synthesize S, N co-doped CDs with red emission for Fe^{3+} and theraonostics [11]. Zhou and co-workers reported a fluorescent probe based on N-doped CDs with red emission for peculiar detection of Pt^{2+}, Au^{3+}, and Pd^{2+} [12]. Chen' group synthesized a colorimetric and fluorescent nanosensor based on B, N, S co-doped CDs (BNS-CDs) with red emission for Fe^{3+} ions in complex biological fluids and living cells [13]. All these results imply the huge biological applications of doped CDs with red emission in sensing, target labeling, and cell imaging.

In recent years, the investigations of biologically crucial cations and thiol-containing amino acids have attracted great attentions due to their unique and important functions in wide range of biological processes [14–18]. Particularly, silver(I) ions (Ag^+), which is one of the most toxic and dangerous heavy metal ions, can pose severe threats to environment and living organisms due to its wide employment in industry [14,19]. Especially, Ag^+ can bind to various metabolites and inactivate sulfhydryl enzymes, causing significant cytopathogenic effects on many kinds of cell types [20,21]. On the other hand, L-cysteine (L-Cys), which is an important biological thiol-containing amino acid, plays an essential and crucial role in maintaining the physiological redox homeostasis [15–17]. Abnormal level of L-Cys in living systems has been correlated with many disease including developmental retardation, encephaledema, liver injuries, and Alzheimer's disease [22,23]. In view of the significances and the considerable concern of Ag^+ and L-Cys, it is of particular interest and great importance to exploit relatively inexpensive, sensitive, and selective approaches for trace amount of Ag^+ and L-Cys in environmental and human samples.

In recent years, several traditional analytical methods have been exploited for Ag^+ and L-Cys, including atomic absorption spectrometry [24], electrochemical technique [25], high performance liquid chromatography [26], and mass spectrometry [27]. However, in general, some of the above methods need time-consuming pretreatments, sophisticated operations, relatively expensive instruments, and relatively poor sensitivity for rapid on-site analysis. Alternatively, a sensitive and specific fluorescence "on-off-on" mode strategy has received considerable attentions and attracted widespread interests. Such fluorescence "on-off-on" mode has been explored to realize simple and sensitive determination of various metal cations and L-Cys. Zong et al. developed a fluorescent CDs probes for "off-on" detection of Cu^{2+} and L-Cys in aqueous solution [16]. Li et al. constructed a fluorescent switch by graphene quantum dots for rapid and label-free dual detection of Hg^{2+} and L-Cys [17]. Huang and co-workers reported a N-doped CDs fluorescent probe for "off-on" detection of Hg^{2+}, L-Cys, and iodide ions [28]. Our group also reported the graphene quantum dot coupled with gold nanoparticle based "off-on" fluorescent probe for L-Cys [29]. Quietly recently, Liao et al. achieved a fluorescence "on-off-on" sensor for Ag^+ and L-Cys based on N-doped CDs [19]. Due to the excellent selectivity in specific targets detection of such "on-off-on" fluorescent sensor, it should be further studied to exploit their potential application in biochemical and biomedical detections.

Herein, we innovatively designed a simple and rapid fluorescence "on-off-on" sensor for Ag^+ and L-Cys in complex biological fluids and living cells based on red emission NBS-CDs. These NBS-CDs were synthesized by a one-step hydrothermal method by using 3-aminobenzeneboronic acid and 2,5-diaminobenzenesulfonic acid as precursors. Due to the co-doping of N, B, and S atoms, these NBS-CDs exhibit excellent optical properties, good biocompatibility, and negligible cytotoxicity on human cells. Moreover, it can be used for the efficient detection of intracellular Ag^+ and L-Cys with excellent biocompatibility and cellular imaging capability, which is regarded as a potential candidate in clinical diagnosis.

2. Experimental section

2.1. Reagents and materials

3-Aminobenzeneboronic acid and 2,5-diaminobenzenesulfonic acid were purchased from Makclin Biochemical Co., Ltd (Shanghai, China). L-Cys and all other biological reagents were obtained from Sigma Reagents Company (St. Louis, MO, USA). Silver nitrate ($AgNO_3$) and all other chemicals were obtained from Aladdin Chemical Reagent Co., Ltd (Shanghai, China). Human cervical carcinoma HeLa cells and human breast carcinoma MCF-7 cells were obtained from Gaining Biological Co., Ltd (Shanghai, China). All other biological reagents for cell culture were purchased from Thermo Fisher Instrument Co., Ltd (Suzhou, China). All reagents were of the highest commercially available purity and were used as received. Ultrapure water with resistivity of 18.2 MΩ cm was produced by passing through a RiOs 8 unit followed by a Millipore-Q Academic purification set (Millipore, Bedford, MA, USA) and was used throughout the whole experiments.

2.2. Synthesis of NBS-CDs

Red emission NBS-CDs were synthesized by the modified hydrothermal methods [13]. Firstly, 0.108 g of 3-aminobenzeneboronic acid and 0.150 g of 2,5-diaminobenzenesulfonic acid were dissolved in 20 mL of ultrapure water, and then the mixture was sonicated for 10 min. The pH of the mixture was mediated to 3.0 by addition of HCl solution (0.1 M). Then, the homogeneous solution was transferred into the Teflon-lined autoclave chamber and heated at 180 °C for 8 h (Figs. S1 and S2). After the reaction, the solution was filtered with 0.22 μm cellulose filter paper to remove large precipitates. The pH of the mixture was mediated to around 7.0 by addition of NaOH solution (0.1 M). Crude product was firstly dialyzed against ultrapure water for 24 h in a dialysis bag with a cut-off molecular weight of 500 Da (Shanghai Green Bird Science & Technology Development Co., China). Then, the solution inside the dialysis bag was further dialyzed against ultrapure water for 48 h through a cut-off molecular weight of 1000 Da (Shanghai Green Bird Science & Technology Development Co., China). The final solution outside the dialysis bag was collected and concentrated to be about 50 mL by rotary evaporation at 65 °C. The final solid NBS-CDs were obtained after vacuum freeze-drying for 48 h and stored at 4 °C for further applications.

2.3. Instruments and characterizations of NBS-CDs

UV-vis absorption spectra were recorded on Shimadzu UV-3600 Plus UV-VIS-NIR spectrophotometer (Shimadzu, Japan). Fluorescence spectra were recorded on Thermo Scientific Lumina

Please cite this article in press as: S. Huang, et al., Red emission nitrogen, boron, sulfur co-doped carbon dots for "on-off-on" fluorescent mode detection of Ag^+ ions and L-cysteine in complex biological fluids and living cells, Analytica Chimica Acta (2018), https://doi.org/10.1016/j.aca.2018.06.051

fluorescence spectrometer (Thermo Fisher Scientific, USA). Time-resolved fluorescence spectra were obtained using the time-correlated single-photo counting (TCSPC) system on Horiba Scientific QM-8075 high sensitivity steady state transient fluorescence spectrometer (HORIBA, Japan). Fourier transform infrared spectroscopy (FT-IR) spectrum was recorded on Thermo Nicolet iS10 spectrometer (Thermo Fisher Scientific, USA). Transmission electron microscopy (TEM) images were taken on Tecnai G2 F20 S-TWIN field emission microscope (FEI, USA). X-ray diffraction (XRD) was recorded on Brucker D-8 Advance Powder X-ray diffractometer (Brucker, Germany). X-ray photoelectron spectroscopy (XPS) data were measured on ESCALAB 250Xi X-ray Photoelectron Spectroscopy (Thermo Fisher Scientific, USA). Elemental analysis was measured on Vario EL/Micro Cube organic element analyzer (Elementar Analysensysteme GmbH, Germany). Confocal fluorescence microscopy images were taken using Nikon A1 confocal laser scanning microscope (Nikon, Japan). The pH values were measured using Sartorius PB-10 pH meter (Sartorius, China).

2.4. Calculation of fluorescent quantum yield and fluorescent lifetime of NBS-CDs

Absolute fluorescent quantum yield (QY) of NBS-CDs was measured using Horiba Scientific QM-8075 high sensitivity steady state transient fluorescence spectrometer (HORIBA, Japan) with excitation wavelength of 520 nm. The absolute fluorescent QY is represented simply by the following equation: $QY = \int L_{emission} / (\int E_{solvent} - \int E_{sample})$ [30]. In this equation, $L_{emission}$ is the photo numbers of the emission spectrum of NBS-CDs, collected using the sphere; E_{sample} and $E_{solvent}$ are the photo numbers of the excitation light used to excite the sample and the solvent (ultrapure water), respectively, collected using the sphere.

Fluorescent lifetime of NBS-CDs was obtained using the time-correlated single-photo counting (TCSPC) system on Horiba Scientific QM-8075 high sensitivity steady state transient fluorescence spectrometer (HORIBA, Japan) with excitation wavelength of 520 nm. Decay traces for the samples were well fitted with the biexponential function based on nonlinear least-squares, according to the reported equations [31].

2.5. Detection of Ag^+ and L-Cys in complex biological fluids

In a typical Ag^+ detection experiment, 100 μL of Ag^+ solution with a concentration ranging from 1 to 1500 μM was added into HEPES buffer (0.02 M, pH 7.0) containing 100 μg/mL of NBS-CDs. The mixture was incubated at room temperature for 3 min. For L-Cys detection, 100 μL of L-Cys solution with a concentration ranging from 0.1 to 500 μM was added into HEPES buffer (0.02 M, pH 7.0) containing 100 μg/mL of NBS-CDs and 400 μM of Ag^+ at room temperature for 2 min. Then, the fluorescence spectra were measured within the wavelength range of 550−750 nm under 520 nm excitation. The band-slits of excitation and emission were all set as 10.0 nm. The fluorescence intensity of NBS-CDs at 605 nm was used for the quantitative analysis of Ag^+ and L-Cys.

For L-Cys detection in real samples, human urine samples and human plasma samples were provided by healthy male and female adult volunteers in our laboratory. All experiments were performed in compliance with the relevant laws and institutional guidelines. Informed consent was obtained from all subjects for all experimentations with human subjects. Informed consent was obtained from all subjects and the experiments were approved by the corresponding Institutional Committee of Guangxi Teachers Education University. Human urine samples were firstly centrifuged at 2000 g for 10 min, and then the filtrate was diluted for a hundred times with HEPES buffer and stored at 4 °C before detection. Human blood samples (1 mL) were centrifuged at 8000 g for 6 min to get rid of blood cells and blood platelet. Then 0.3 mL of acetonitrile was added into plasma solution to precipitate proteins with vigorous stirring. After incubation for 20 min, the solution was centrifuged at 8000 g for 20 min, and then supernatant was transferred into a 2 mL Eppendorf tube. The pretreated human plasma samples were diluted for fifty times with HEPES buffer and stored at 4 °C before detection [32]. The concentrations of L-Cys in human urine samples and human plasma samples were calculated using the calibration curve obtained in aqueous buffer.

2.6. Detection of Ag^+ and L-Cys in living cells

Firstly, the cytotoxicity of NBS-CDs on HeLa cells and MCF-7 cells were investigated by MTT [3-(4,5-dimethylthiazol-2-yl)-2,5-diphenyltetra-zolium bromide] assay. All cells were seeded in 96-well plates in Dulbecco's modified eagle medium (DMEM) medium (10% FBS and 1% penicillin-streptomycin) and cultured at 37 °C in a humidified 5% CO_2 for 24 h. Then, different concentrations of NBS-CDs (0, 20, 30, 60, 100, 200, and 300 μg/mL) were added into the cells for further incubation at 37 °C for 24 h and 48 h, respectively. Then, 20 μL of MTT (5 mg/mL) was added into each well and the cells were incubated for additional 4 h. The culture medium was removed, and the mixtures were dissolved in 200 μL of dimethyl sulfoxide (DMSO) with continuous shaking for 10 min. The optical density (OD) of the purple formazan in each well at 490 nm was measured using an enzyme-linked immunosorbent assay (ELISA) plate reader with pure DMSO as the blank. The cytotoxicity is calculated by this equation: cell viability (%) = $OD_{treated}/OD_{control} \times 100$, where $OD_{control}$ and $OD_{treated}$ are the OD of the cells before and after the treatment with NBS-CDs, respectively. Results were expressed as their mean standard deviations of six replicate experiments.

For detection of Ag^+ and L-Cys in living cells, HeLa cells and MCF-7 cells were seeded onto 35 mm glass bottom culture dishes and grown in DMEM medium (10% FBS and 1% penicillin-streptomycin) with a humidified atmosphere containing 5% CO_2 at 37 °C for 24 h. Then, the culture medium was discarded and the cells were incubated with 2 mL of NBS-CDs (100 μg/mL) for another 6 h. For imaging of living cells treated with Ag^+, the cells were incubated with 2 mL of NBS-CDs (100 μg/mL) before or after treating with different concentrations of Ag^+ for 5 min. For imaging of living cells treated with Ag^+ and L-Cys, the cells were incubated with 2 mL of NBS-CDs (100 μg/mL) and Ag^+ (400 μM) before or after treating with different concentrations of L-Cys for 8 min. After the incubation, the cells were washed with HEPES buffer (0.02 M, pH 7.0) for three times. Confocal microscopy images were immediately captured at room temperature on a laser scanning confocal microscopy (Nikon A1, Japan) using a digital camera.

3. Results and discussions

3.1. Characterization of NBS-CDs

As shown in Fig. 1a, NBS-CDs are almost spherical in shape and monodisperse in water without apparent aggregation. As further shown in the insert of Fig. 1a, high resolution TEM image taken from one particle dot shows an obvious lattice spacing of 0.21 nm, which is attributed to the in-plane lattice spacing of graphene structure (100 facet) [33]. Based on the statistical analysis of more than one hundred particles, these NBS-CDs displays the size distribution between 1.5 nm and 4.0 nm with an average size of 2.84 nm (Fig. 1b). Further shown in Fig. 1c, NBS-CDs exhibits broad 2θ patterns at around 24.1° and 42° which are ascribed to disordered carbon atoms with the lattice spacing of 002 facet and 100

Please cite this article in press as: S. Huang, et al., Red emission nitrogen, boron, sulfur co-doped carbon dots for “on-off-on” fluorescent mode detection of Ag^+ ions and L-cysteine in complex biological fluids and living cells, Analytica Chimica Acta (2018), https://doi.org/10.1016/j.aca.2018.06.051

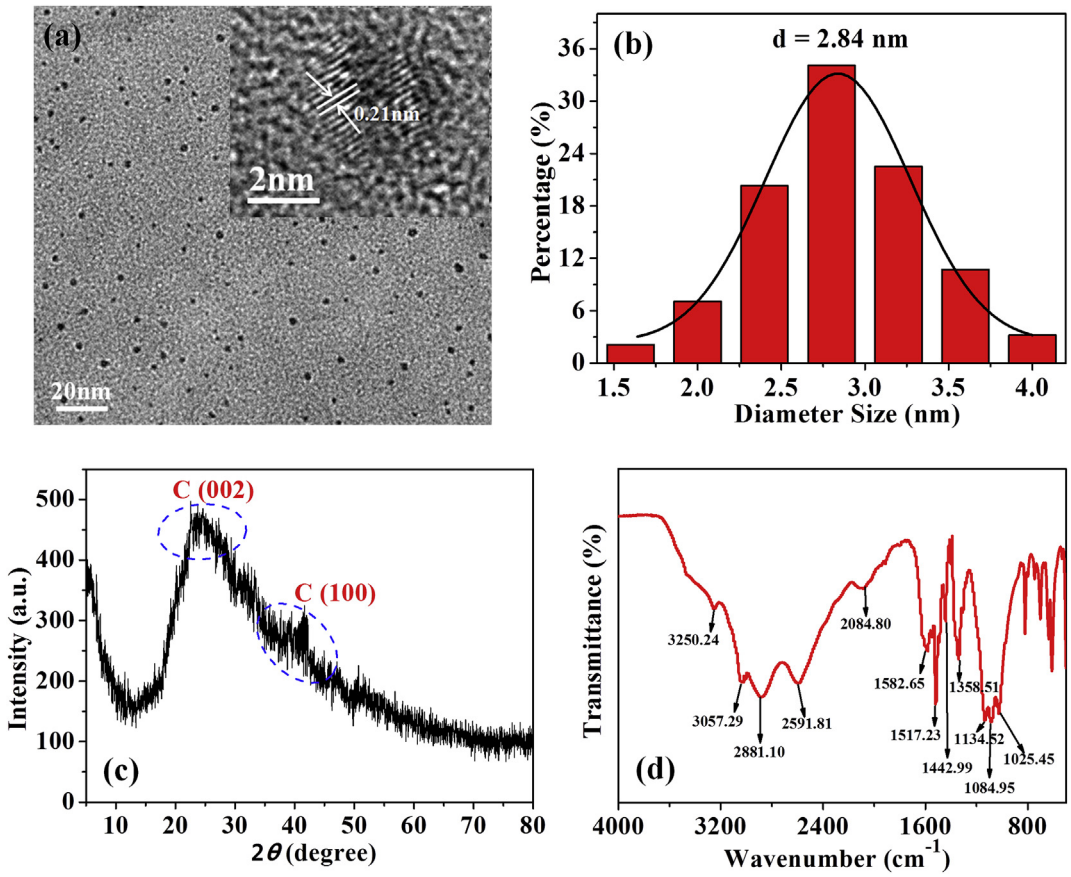

Fig. 1. (a) Typical TEM images of NBS-CDs. Insert: magnification of a single nanoparticle. (b) Diameter size distribution curve of NBS-CDs. (c) XRD spectrum of NBS-CDs. (d) FT-IR spectrum of NBS-CDs.

facet for the high degree graphitization of NBS-CDs [9,34]. The XRD peak at 24.1° of NBS-CDs is corresponding to an interlayer spacing of 0.37 nm that is a little larger than the interlayer spacing in graphite of 0.34 nm, attributing to the introduction of more surface-attached amine or amido moieties [35]. Such NBS-CDs can be used as fluorescent probes for transporting the efficient and therapeutic moieties for targeted drug delivery.

Functional groups of NBS-CDs were further characterized by FT-IR spectrometry. As shown in Fig. 1d, the absorption peaks from 3500 cm^{-1} and 3000 cm^{-1} are attributed to the characteristic vibration bands of O–H and N–H bonds on the surface of the NBS-CDs [36]. Broad absorption peaks at 2881.10 cm^{-1} and 2591.81 cm^{-1} are assigned to the bending and stretching vibrations of C–H and S–H bonds, respectively [37]. A new obvious peak appeared at 2084.80 cm^{-1} is assigned to the –SCN– group [11]. Three sharp and distinct absorption peaks at 1582.62 cm^{-1}, 1517.23 cm^{-1}, and 1442.99 cm^{-1} are resulted from the stretching vibrations of C=O, C=C, and C–N bonds, respectively [11,13]. The absorption peak at 1358.51 cm^{-1} is ascribed to the stretching vibration of C–C, C–S, C–O–C, and B–O bonds, respectively [9,38]. Three tight absorption peaks at 1134.52 cm^{-1}, 1084.95 cm^{-1}, and 1025.45 cm^{-1} are assigned to the B–O–H bending vibration, C–B stretching vibration, and the B–O–H deformation vibration, respectively [13,39]. All these absorption peaks suggest the successful doping of N, B, and S atoms in the prepared NBS-CDs.

More detail elemental contents and surface composition of NBS-CDs were investigated by XPS spectra. As shown in Fig. 2a, the full survey XPS spectrum of NBS-CDs clearly exhibits five typical peaks at 168.19 eV, 191.24 eV, 284.82 eV, 401.32 eV, and 531.36 eV, which are attributed to the characteristic binding energy signals of S 2p, B 1s, C 1s, N 1s, and O 1s, respectively. EDS spectrum further confirms the existences of S, B, C, N, and O elements (Fig. S3). The elemental analysis indicates the composition of NBS-CDs as C 35.38 wt %, H 5.12 wt %, N 11.47 wt %, B 6.25 wt %, S 10.15 wt %, and O (calculated) 31.63 wt % (Table S1a). According to the results of elemental analysis, the empirical formula of NBS-CDs is calculated to be approximately $C_{37}H_{64}N_{10}B_7S_4O_{25}$ (Table S1b). The high-resolution C 1s spectrum indicates the presence of C–B (283.89 eV), C–C/C=C (284.78 eV), C–O/C–S (285.55 eV), and C–N/C–O (286.00 eV), respectively (Fig. 2b) [34,40]. The high-resolution N 1s spectrum shows three dominant peaks at 401.95 eV, 401.20 eV, and 399.48 eV which are assigned to N–H, C–N, and C–N–C, respectively (Fig. 2c) [9,41]. The high-resolution B 1s spectrum shows three peaks at 192.23 eV, 191.10 eV, and 190.43 eV, assigned to B–S, B–O, and B–C, respectively (Fig. 2d) [9]. The high-resolution S 2p spectrum shows three peaks (Fig. 2e): the peaks at 167.90 eV and 168.45 eV correspond to S $2p^{3/2}$ and S $2p^{1/2}$ spectra of the C–S–C covalent bond [11], another peak at higher energy (167.9 eV) is assigned to –C–SOx– (x = 2, 3, and 4) species [42]. The high-resolution O 1s spectrum also shows three peaks at 532.93 eV, 532.08 eV, and 531.15 eV, assigned to O=C–O, C–O, and C=O, respectively (Fig. 2f) [43]. The results of FT-IR and XPS spectra confirm that N, B, and S atoms are perfectly co-doped in CDs, and some related functional groups (hydroxyl, carboxyl, and amino groups) are existed on the surface of NBS-CDs.

Please cite this article in press as: S. Huang, et al., Red emission nitrogen, boron, sulfur co-doped carbon dots for “on-off-on” fluorescent mode detection of Ag^+ ions and L-cysteine in complex biological fluids and living cells, Analytica Chimica Acta (2018), https://doi.org/10.1016/j.aca.2018.06.051

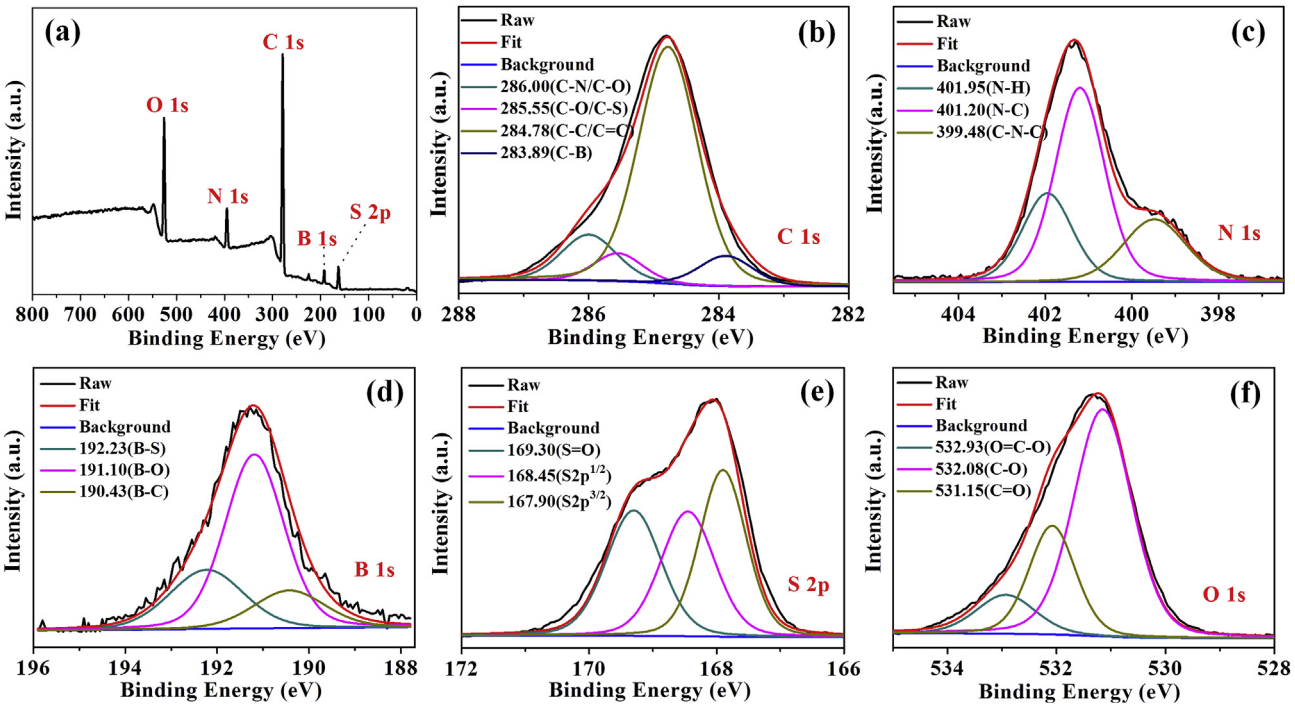

Fig. 2. XPS survey spectrum (a), C 1s XPS spectrum (b), N 1s XPS spectrum (c), B 1s XPS spectrum (d), S 2p XPS spectrum (e), and O 1s XPS spectrum (f) of NBS-CDs.

3.2. Optical properties of NBS-CDs

Optical properties of NBS-CDs were investigated by UV-vis absorption spectrometry and fluorescence spectrometry. As shown in Fig. 3a, NBS-CDs exhibit two typical absorption peaks at 234 nm and 286 nm, respectively, resulting from the $\pi \rightarrow \pi^*$ electronic transition of the aromatic sp^2 carbon in NBS-CDs [33]. Furthermore, the maximum excitation and emission peaks of NBS-CDs are located at 520 nm and 605 nm, respectively. Under the excitation of a hand-held UV lamp with 365 nm, the light red NBS-CDs aqueous solution emits a bright red fluorescence (insert in Fig. 3a). The Commission International d'Eclairage (CIE) 1931 2° chromaticity diagram [44] shows that these NBS-CDs emit red light with CIE color coordinates of CIE 1931: (x, y)=(0.6027, 0.3966) and CIE 1976: (u', v')=(0.3678, 0.5446) (Fig. S4). However, unlike most reported CDs, these NBS-CDs shows an excitation wavelength-independent feature during the range of the excitation wavelength. As shown in Fig. 3b, when the excitation wavelength increases from 410 nm to 530 nm, the emission wavelength of NBS-CDs is independent of the excitation wavelength. It can be speculated that the doping of N, B, and S atoms can mediate both the sizes and the surface states of CDs, resulting in the relative uniform size distribution and surface state of NBS-CDs [13].

To evaluate the optical stability of NBS-CDs, the influences of longtime irradiation by UV light, pH value, and ionic strength on their fluorescence intensity were investigated. The preliminary experimental results showed that the fluorescence intensity of NBS-CDs was not significantly changed even under continuous irradiation of 365 nm UV light for 90 min (Fig. S5), wide range of pH values from 3 to 8 (Fig. S6), and ultrahigh concentration of NaCl solution (1.5 M) (Fig. S7). According to the TCSPC system, the average fluorescence lifetime of NBS-CDs (excited at 520 nm) was calculated to be around 1.35 ns (Fig. S8). The absolute fluorescence QY of NBS-CDs (excited at 520 nm) was calculated to be 11.6% by using the integrating sphere, which was two times higher than the reported NBS-CDs by using 4-aminobenzeneboronic acid as the

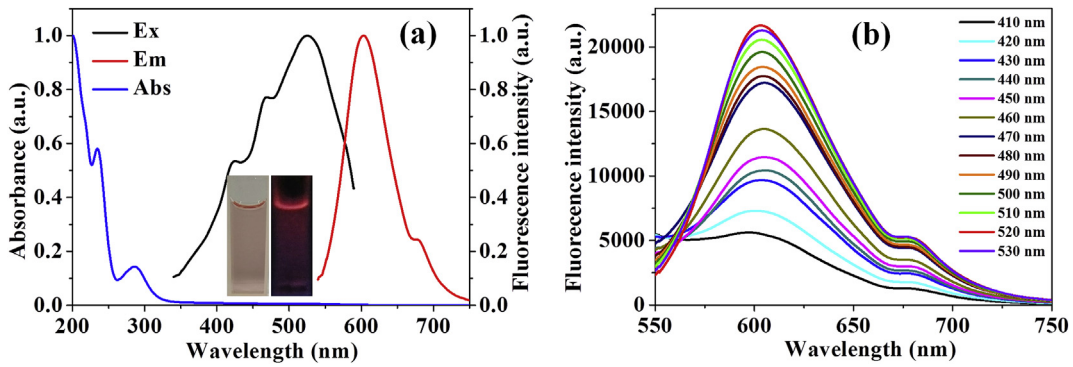

Fig. 3. (a) UV-vis absorption spectrum of NBS-CDs, excitation spectrum of NBS-CDs at $\lambda_{em} = 605$ nm, and emission spectrum of N,B-CDs at $\lambda_{ex} = 520$ nm. Insert: Photograph of NBS-CDs under the excitation of white light (Left) and UV lamp with 365 nm (Right). (b) Fluorescence spectra of NBS-CDs with the excitation wavelength increasing from 410 nm to 530 nm.

Please cite this article in press as: S. Huang, et al., Red emission nitrogen, boron, sulfur co-doped carbon dots for "on-off-on" fluorescent mode detection of Ag^+ ions and L-cysteine in complex biological fluids and living cells, Analytica Chimica Acta (2018), https://doi.org/10.1016/j.aca.2018.06.051

reactant [13]. Therefore, the as-prepared NBS-CDs with excellent fluorescence property even under extremely harsh conditions facilitates their potential biological applications in sensing, analysis, and cells imaging.

3.3. Detection mechanism of Ag^+ and L-Cys

Such NBS-CDs are found to display an interesting "on-off-on" three-state emission with the stepwise addition of Ag^+ and L-Cys. As illustrated in a proposed sensing process of Scheme 1, the fluorescence of NBS-CDs can be quenched by Ag^+ due to its chelation with NBS-CDs, which facilitates the charge transfer from the excited state of NBS-CDs to Ag^+ [32]. Due to the stronger binding interaction of Ag^+ with L-Cys, Ag^+ can be taken away from the surface of NBS-CDs after the addition of L-Cys [15,32]. During this process, the fluorescence of NBS-CDs changes from "on" to "off" and then "on" again. The interactions among NBS-CDs, Ag^+, and L-Cys were confirmed by UV-vis absorption spectrometry and the fluorescence lifetime experiment. As shown in Fig. 4a, the absorption peaks of NBS-CDs shift to the longer wavelength (from 520 nm to 655 nm) after the addition of 400 μM of Ag^+, which proves that Ag^+ indeed complexes with NBS-CDs (insert in Fig. 4a). When 400 μM of L-Cys is present, the absorption peaks of NBS-CDs shift to its former position again. Further shown in Fig. 4b, the average fluorescence lifetime of pure NBS-CDs is calculated to be 1.35 ns, consisting of a short lifetime component of 1.24 ns (86.88%) and a long lifetime component of 3.53 ns (13.12%). However, the presences of 400 μM of Ag^+ and 400 μM of L-Cys can not vary the average fluorescence lifetime of NBS-CDs significantly (insert in Fig. 4b). Since the average fluorescence lifetime of NBS-CDs remains almost constant before or after the addition of Ag^+, the fluorescence quenching mechanism of NBS-CDs/Ag^+ system is static fluorescence quenching process [29]. All these findings make the as-prepared NBS-CDs behave as a potentially bifunctional sensor for the recognition of Ag^+ and L-Cys.

3.4. Detection of Ag^+ and L-Cys in complex biological fluids

Based on the fluorescence "on-off-on" mode of NBS-CDs/Ag^+/L-Cys system, NBS-CDs can be used as the fluorescent sensor for the determination of Ag^+ and L-Cys with good selectivity and high sensitivity. In order to obtain the best sensing response, some analytical parameters were optimized systematically: (a) Amount of NBS-CDs; (b) Concentration of Ag^+; (c) pH value of HEPES buffer; (d) Reaction time of NBS-CDs/Ag^+ system; (e) Reaction time of NBS-CDs/Ag^+/L-Cys system. As shown in Figs. S9 and S10, the below optimal analytical parameters are found to get the best result: (a) Amount of NBS-CDs of 0.1 mg/mL; (b) Concentration of Ag^+ of 400 μM; (c) HEPES buffer with pH 7.0; (d) Reaction time of NBS-CDs/Ag^+ system of 3 min; (e) Reaction time of NBS-CDs/Ag^+/L-Cys system of 2 min.

Under the optimal conditions, the Ag^+ solution with different concentrations was added into the NBS-CDs solution and then the fluorescence spectra were recorded to investigate the sensitivity of this sensor. As exhibited in Fig. 5a, the fluorescence intensity of NBS-CDs decreases dramatically with the increasing concentration of Ag^+. The relationship between the relative fluorescence intensity of NBS-CDs and the concentration of Ag^+ was also investigated (Fig. 5b). It is obvious that the relative fluorescence intensity of NBS-CDs displays a good linear relationship to the concentration of Ag^+ in the range from 1 μM to 300 μM with a good correlation coefficient of 0.9987. The fitted linear regression equation is $I_0/I = 5.13 \times 10^3 \times [Ag^+]\ (\mu M) + 1$, where I_0 and I are the fluorescence intensities of NBS-CDs in the absence and presence of Ag^+, respectively. The limit of detection for Ag^+ is calculated to be 0.35 μM according to the three times signal-to-noise criteria.

This fluorescent sensing assay can be further applied to detect L-Cys. When L-Cys is added into the NBS-CDs/Ag^+ system, the level of the fluorescence quenching of NBS-CDs is limited in proportion to the concentration of L-Cys. As shown in Fig. 6a, it is clear that the fluorescence of NBS-CDs is recovered gradually with increasing concentration of L-Cys. Fig. 6b shows the relationship between the relative fluorescence intensity of NBS-CDs and the concentration of L-Cys. It is obvious that the relative fluorescence intensity of NBS-CDs shows a good linear relationship to the concentration of L-Cys in the range from 0.1 μM to 20 μM with a good correlation coefficient of 0.9974 (insert in Fig. 6b). The fitted linear regression equation is $I/I_0 = 4.30 \times 10^4 \times [\text{L-Cys}]\ (\mu M) + 1.16$, where I_0 and I stand for the fluorescence intensities of NBS-CDs/Ag^+ system in the absence and presence of L-Cys, respectively. The limit of detection for L-Cys is calculated to be 0.045 μM according to the three times signal-to-noise criteria, suggesting the ultrahigh sensitivity of this fluorescent sensing assay. Comparing the performance of the prepared NBS-CDs with the previously reported probes for L-Cys (Table S2), the sensitivity of this sensor was superior. To further evaluate the practical application of this fluorescent sensing assay, this NBS-CDs-based fluorescent sensor was applied for the determination of L-Cys in human urine samples and human plasma samples. As shown in Table S3, good recoveries and high analytical precision were obtained in the diluted samples with various concentrations of standard L-Cys solution. These results confirm the reliability and the feasibility of such NBS-CDs-based fluorescent sensor for monitoring L-Cys in biological samples.

To evaluate the selectivity of the proposed method, the effects of some potential interferences from common ions for Ag^+ detection were investigated. As exhibited in Fig. 7a, most common ions, except Fe^{3+}, can hardly cause significant alteration on the fluorescence intensity of NBS-CDs. It has been reported that tartaric acid

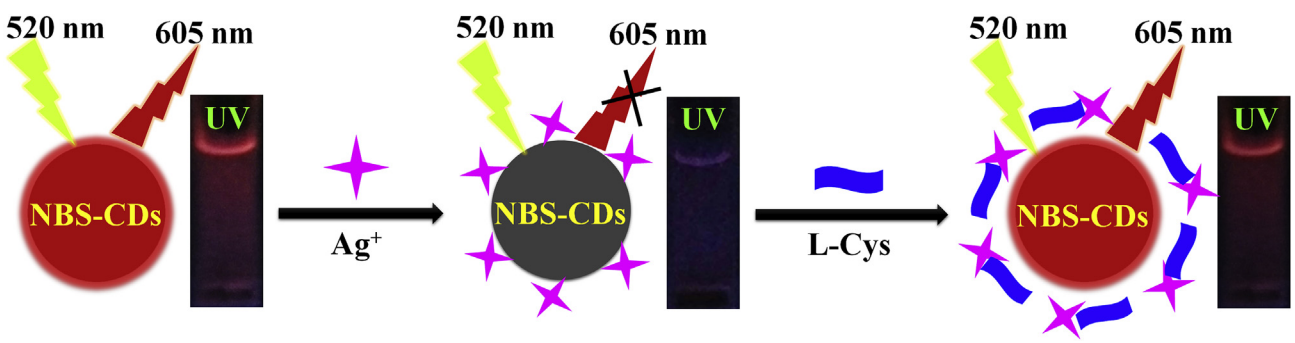

Scheme 1. Schematic illustration of Ag^+ and L-Cys determinations.

Please cite this article in press as: S. Huang, et al., Red emission nitrogen, boron, sulfur co-doped carbon dots for "on-off-on" fluorescent mode detection of Ag^+ ions and L-cysteine in complex biological fluids and living cells, Analytica Chimica Acta (2018), https://doi.org/10.1016/j.aca.2018.06.051

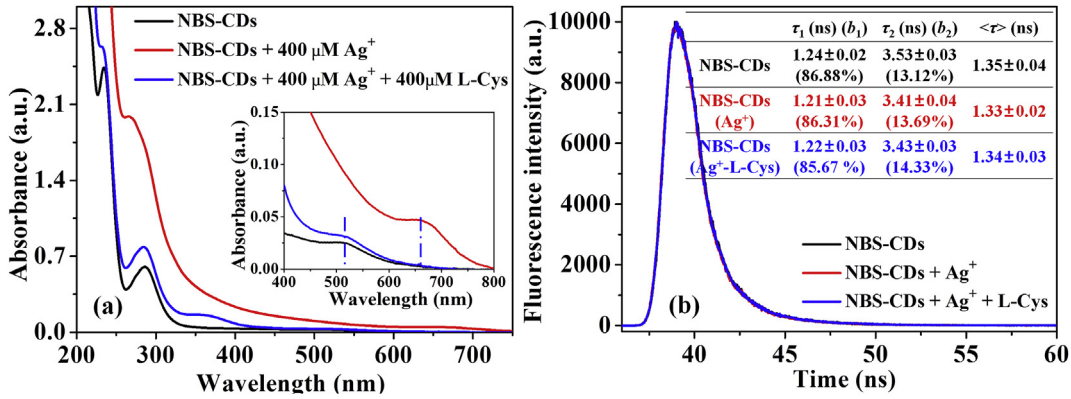

Fig. 4. (a) UV-vis absorption spectra of NBS-CDs, Ag^+, and L-Cys system. (b) Fluorescence decay trace of NBS-CDs after the addition of Ag^+ and L-Cys. The measurement is made at $\lambda_{em} = 520$ nm τ is the fluorescence lifetime of NBS-CDs, and b is the normalized preexponential factor, respectively.

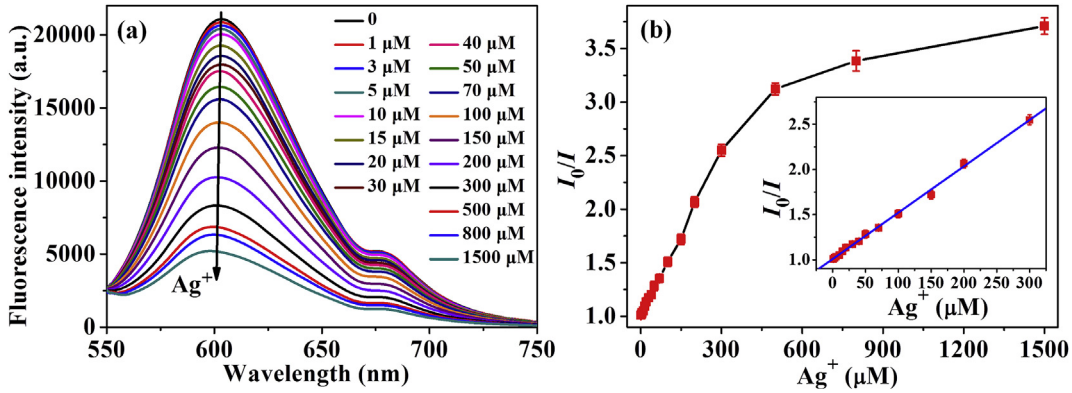

Fig. 5. (a) Fluorescence spectra of NBS-CDs (100 μg/mL) after the addition of different concentration of Ag^+. (b) Relationship between the relative fluorescence intensity of NBS-CDs and concentration of Ag^+ from 1 μM to 1500 μM. Insert: Linear relationship between the relative fluorescence intensity of NBS-CDs and concentration of Ag^+ from 1 μM to 300 μM.

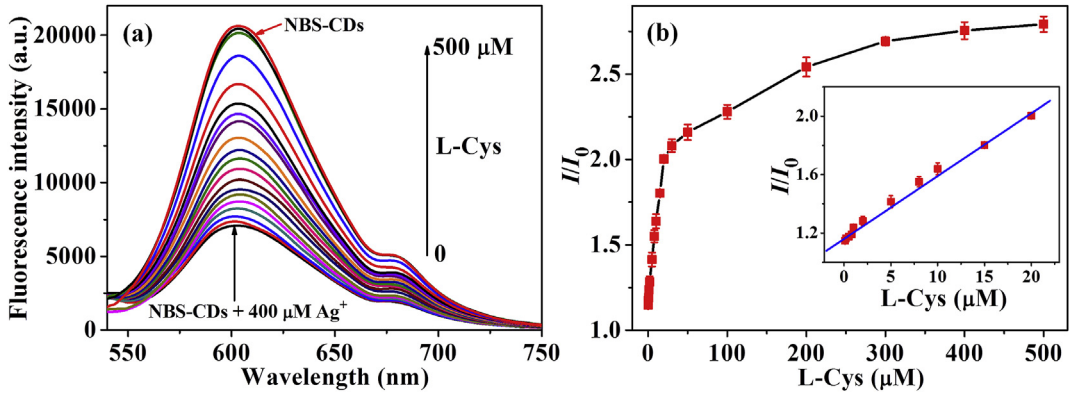

Fig. 6. (a) Fluorescence spectra of NBS-CDs (100 μg/mL) and Ag^+ (400 μM) after the addition of different concentration of L-Cys. (b) Relationship between the relative fluorescence intensity of NBS-CDs and concentration of L-Cys from 0.1 μM to 500 μM. Insert: Linear relationship between the relative fluorescence intensity of NBS-CDs and concentration of L-Cys from 0.1 μM to 20 μM.

and ascorbic acid are widely used as the masking agent for Fe^{3+} [45]. Herein, the interference from Fe^{3+} on the fluorescence intensity of NBS-CDs was effectively eliminated by the addition of tartaric acid and ascorbic acid (line M-Fe^{3+} in Fig. 7a). Moreover, Cr(VI) exhibits almost no interference on the fluorescence intensity of NBS-CDs. Therefore, this method can realize the selective determination of Ag^+. On the other hand, the interferences of some biological substances in organisms including common ions, carbohydrates, and some important amino acids, were investigated. It can be seen from Fig. 7b that none of these interferents cause obvious fluorescence alterations. Although higher concentrations of other thiol-containing molecules, such as glutathione (GSH) and homocysteine (Hcy), can actually induce a certain amount of fluorescence restoration of the NBS-CDs/Ag^+ system, the levels of L-Cys in human plasma are much higher than those of GSH and Hcy (ca. 20- to 50-fold) [46]. Therefore, the ensemble of NBS-CDs and Ag^+ can be implemented as a selective sensing platform for L-Cys in human plasma samples. All these results demonstrate that the NBS-

Please cite this article in press as: S. Huang, et al., Red emission nitrogen, boron, sulfur co-doped carbon dots for "on-off-on" fluorescent mode detection of Ag^+ ions and L-cysteine in complex biological fluids and living cells, Analytica Chimica Acta (2018), https://doi.org/10.1016/j.aca.2018.06.051

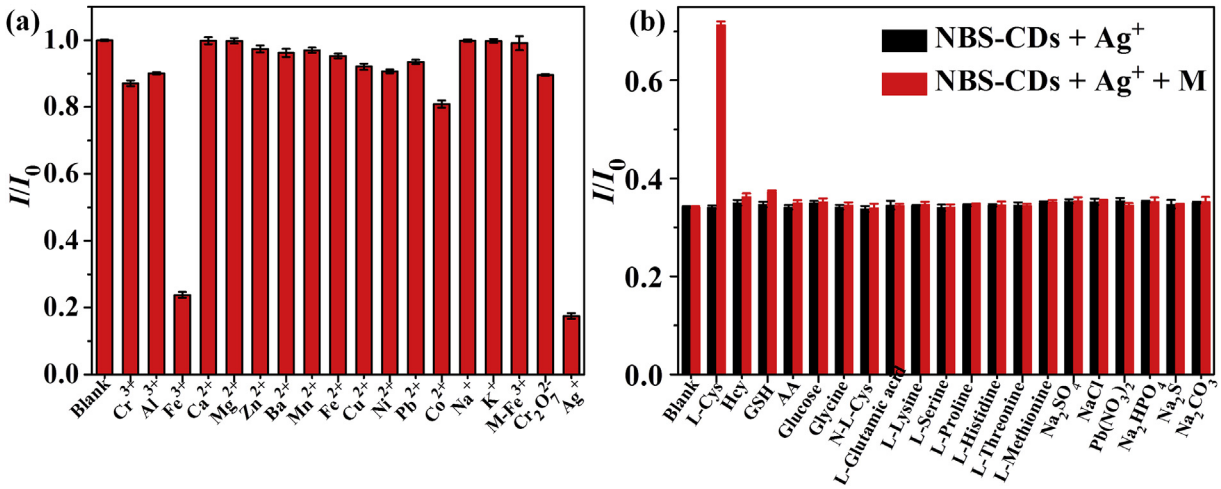

Fig. 7. (a) Influences of some common ions (2 mM) on the fluorescence intensity of NBS-CDs (100 μg/mL). M-Fe^{3+}: 2 mM Fe^{3+}, 600 μM tartaric acid, and 600 μM ascorbic acid. (b) Influences of common ions, carbohydrates, and some important amino acids on the fluorescence intensity of NBS-CDs/Ag^+ system. Concentrations of GSH and Hcy were 5 μM; Concentrations of AA, N-L-Cys, and glucose were 100 μM; Concentrations of others were 1 mM.

CDs are potentially employed as a high selective sensor for Ag^+ and L-Cys.

3.5. Detection of Ag^+ and L-Cys in living cells

To evaluate the potential applications of NBS-CDs for intercellular detection of Ag^+ and L-Cys, the cytotoxicity and biocompatibility of these NBS-CDs were investigated through their incubation with HeLa cells and MCF-7 cells by MTT assays. It seemed that over 80% cell viability was observed after incubating HeLa cells and MCF-7 cells with NBS-CDs (from 0 to 300 μg/mL) even for 24 h and 48 h (Fig. S11), so these NBS-CDs exhibit negligible cytotoxicity and good biocompatibility to living cells. Furthermore, in order to investigate the influence of these NBS-CDs on the cellular morphology, the images of HeLa cells and MCF-7 cells pre-incubated with NBS-CDs were taken by laser scanning confocal microscopy. When HeLa cells and MCF-7 cells were incubated with 300 μg/mL of NBS-CDs at 37 °C for 4 h, the shape and the structure of these cells were remained and a significant red emission from the intracellular region was observed (Fig. S12), demonstrating the feasibility of these NBS-CDs in living cells imaging.

To further investigate the applicability of these NBS-CDs for intracellular monitoring Ag^+ and L-Cys levels, Ag^+ and L-Cys solution with different concentrations were introduced into the NBS-CDs pretreated cells. The cells were washed with HEPES buffer (0.02 M, pH 7.0) for three times and then the confocal microscopy images were immediately captured using a digital camera. It is observed that NBS-CDs exhibit strong red emission in the inside of these two cells (Fig. 8a, 8a', 9a, and 9a'). As further shown in Figs. 8 and 9, the red emission of NBS-CDs is weakened gradually with the increase of the Ag^+ concentration. The red fluorescence of NBS-CDs decreases obviously even in the present of small concentration of Ag^+ (10 μM), suggesting the high sensitivity of these NBS-CDs for Ag^+ detection. On the other hand, L-Cys can efficiently recover the fluorescence of NBS-CDs. As shown in Figs. 10 and 11, with the increasing concentration of L-Cys, the red fluorescence of NBS-CDs is restored to the control emission. The red fluorescence of NBS-CDs increases distinctly even in the present of 1 μM of L-Cys, further implying the good sensitivity of these NBS-CDs/Ag^+ system for L-Cys determination. All these results suggest that the as-prepared

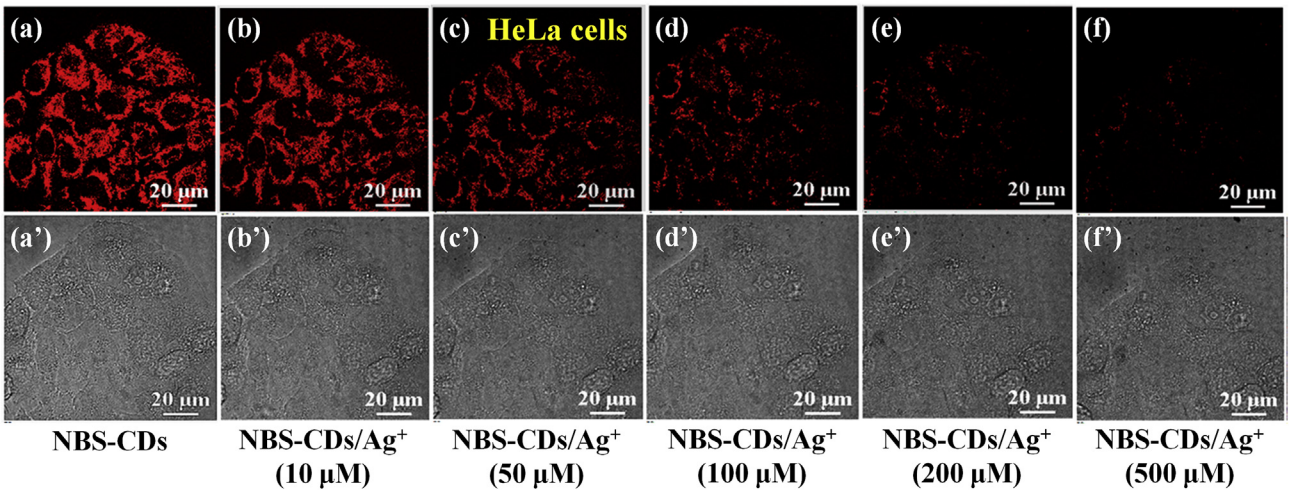

Fig. 8. Confocal fluorescence images (a–f) and bright fields images (a'-f') of HeLa cells incubated with NBS-CDs (100 μg/mL) before or after the addition of Ag^+ with different concentrations at 37 °C for 5 min.

Please cite this article in press as: S. Huang, et al., Red emission nitrogen, boron, sulfur co-doped carbon dots for "on-off-on" fluorescent mode detection of Ag^+ ions and L-cysteine in complex biological fluids and living cells, Analytica Chimica Acta (2018), https://doi.org/10.1016/j.aca.2018.06.051

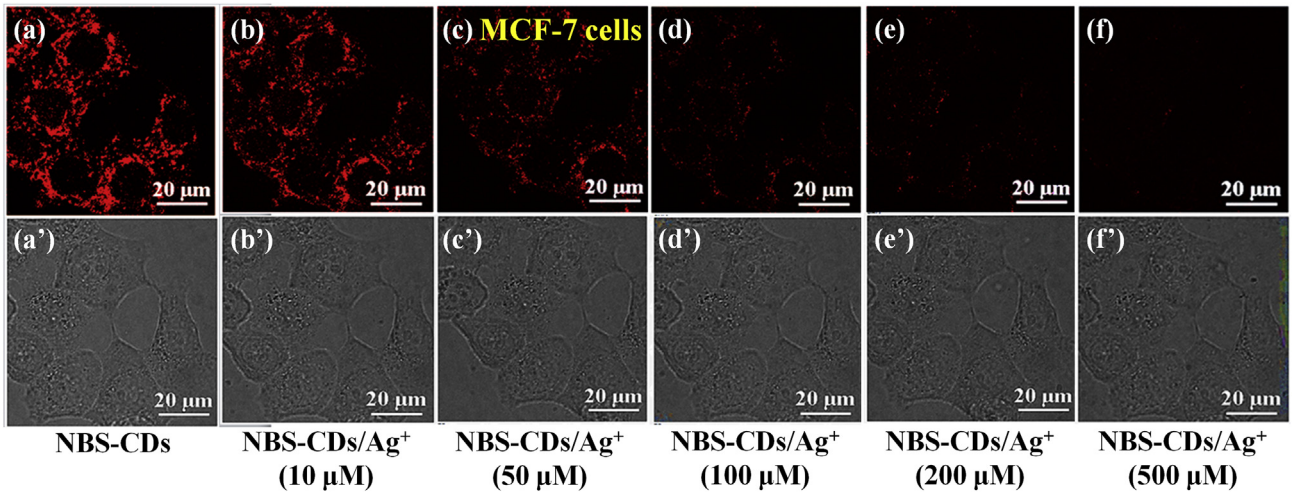

Fig. 9. Confocal fluorescence images (a–f) and bright fields images (a'-f') of MCF-7 cells incubated with NBS-CDs (100 μg/mL) before or after the addition of Ag^+ with different concentrations at 37 °C for 5 min.

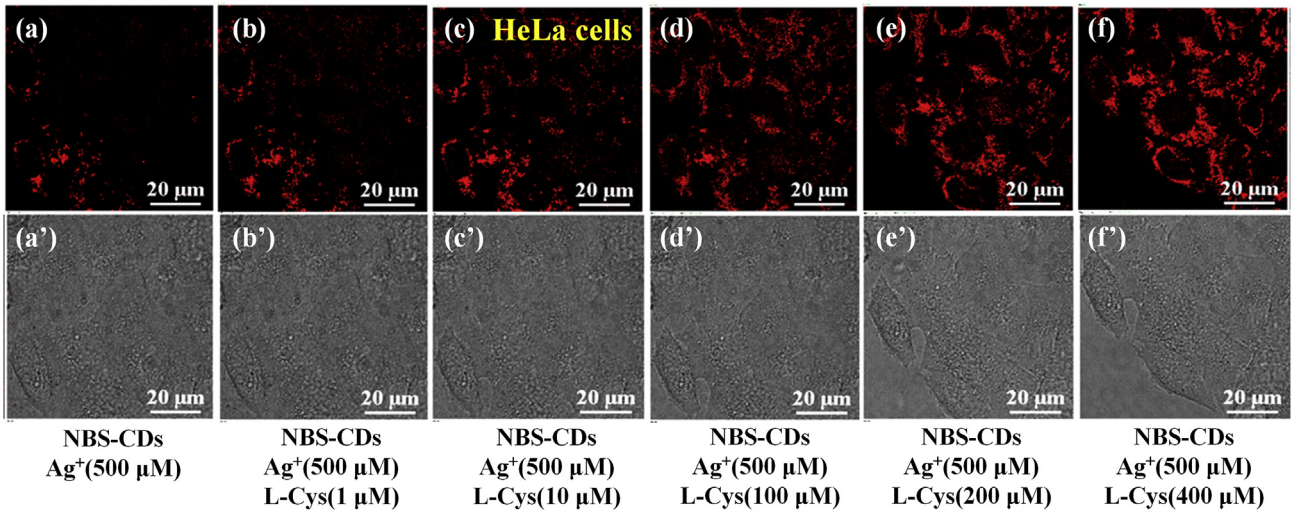

Fig. 10. Confocal fluorescence images of HeLa cells incubated with NBS-CDs (100 μg/mL) and Ag^+ (500 μM) before or after the addition of L-Cys with different concentrations at 37 °C for 8 min.

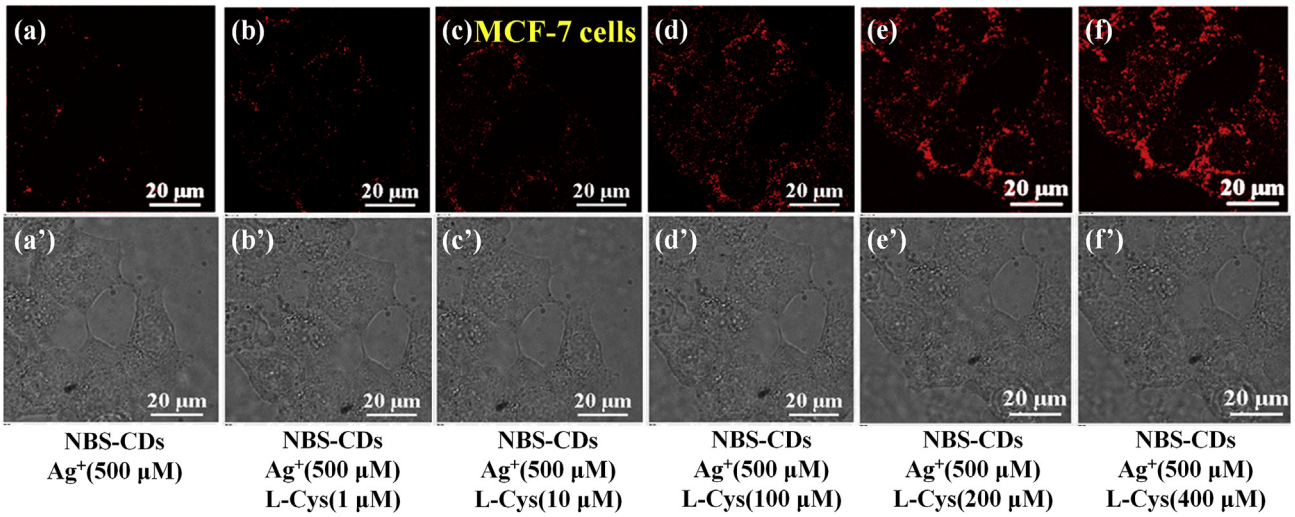

Fig. 11. Confocal fluorescence images of MCF-7 cells incubated with NBS-CDs (100 μg/mL) and Ag^+ (500 μM) before or after the addition of L-Cys with different concentrations at 37 °C for 8 min.

Please cite this article in press as: S. Huang, et al., Red emission nitrogen, boron, sulfur co-doped carbon dots for "on-off-on" fluorescent mode detection of Ag^+ ions and L-cysteine in complex biological fluids and living cells, Analytica Chimica Acta (2018), https://doi.org/10.1016/j.aca.2018.06.051

NBS-CDs can be used for intracellular determinations of Ag^+ and L-Cys with the naked eyes. Therefore, these NBS-CDs are promising low cytotoxicity, super biocompatibility, and excellent fluorescent labeling agents for cellular imaging in the optical window.

4. Conclusions

In summary, NBS-CDs-based fluorescent "on-off-on" sensor for Ag^+ and L-Cys in complex biological fluids and living cells was developed. Due to co-doping of N, B, and S atoms, NBS-CDs show excellent optical property, good fluorescent stability, favorable biocompatibility, and low cytotoxicity on HeLa cells and MCF-7 cells. These red emission NBS-CDs were used for highly selective and sensitive detections of Ag^+ and L-Cys with detection limits as low as 0.35 μM and 0.045 μM, respectively. Especially, some common ions, carbohydrates, and important amino acids did not affect the detections of Ag^+ and L-Cys. The proposed NBS-CDs-based sensing strategy was proven to be a simple and efficient method for fluorescent "on-off-on" determination mode, which provided an efficient platform for desirable biological applications in analytical areas.

Acknowledgements

This work was financially supported by National Natural Science Foundation of China (21763005, 21563006), Natural Science Foundation of Guangxi Province (2017GXNSFDA198034, 2017GXNSFFA198005, 2016GXNSFBA380118, 2015GXNSFAA139033), Guangxi Scientific and Technological Development Projects (1598025-8, AD17195081), the High-Level-Innovation Team (guijiaoren[2017]38) and Outstanding Scholar Project of Guangxi Higher Education Institutes, and BAGUI Scholar Program of Guangxi Province of China.

Appendix A. Supplementary data

Supplementary data related to this article can be found at https://doi.org/10.1016/j.aca.2018.06.051.

References

[1] G.A.M. Hutton, B.C.M. Martindale, E. Reisner, Carbon dots as photosensitisers for solar-driven catalysis, Chem. Soc. Rev. 46 (2017) 6111–6123.
[2] P. Namdari, B. Negahdari, A. Eatemadi, Synthesis, properties and biomedical applications of carbon-based quantum dots: an updated review, Biomed. Pharmacother. 87 (2017) 209–222.
[3] X.Y. Zhang, M.Y. Jiang, N. Niu, Z.J. Chen, S.J. Li, S.X. Liu, J. Li, Natural-product-derived carbon dots: from natural products to functional materials, ChemSusChem 11 (2018) 11–24.
[4] Q. Xu, T.R. Kuang, Y. Liu, L.L. Cai, X.F. Peng, T.S. Sreeprasad, P. Zhao, Z.Q. Yu, N. Li, Heteroatom-doped carbon dots: synthesis, characterization, properties, photoluminescence mechanism and biological applications, J. Mater. Chem. B 4 (2016) 7204–7219.
[5] Y.F. Zhang, M. Park, H.Y. Kim, B. Ding, S.J. Park, A facile ultrasonic-assisted fabrication of nitrogen-doped carbon dots/BiOBr up-conversion nanocomposites for visible light photocatalytic enhancements, Sci. Rep. 7 (2017) 45086.
[6] Q. Xiao, Y. Liang, F.W. Zhu, S.Y. Lu, S. Huang, Microwave-assisted one-pot synthesis of highly luminescent N-doped carbon dots for cellular imaging and multi-ion probing, Microchim. Acta 184 (2017) 2429–2438.
[7] Y. Huang, Z.J. Cheng, Simple and green synthesis of boron-, sulfur-, and nitrogen-co-doped carbon dots as fluorescent probe for selective and sensitive detection of sunset yellow, Nano 12 (2017) 1750123.
[8] X.B. Cui, Y.L. Wang, J. Liu, Q.Y. Yang, B. Zhang, Y. Gao, Y. Wang, G.Y. Lu, Dual functional N- and S-co-doped carbon dots as the sensor for temperature and Fe^{3+} ions, Sensor. Actuator. B Chem. 242 (2017) 1272–1280.
[9] T. Tian, Y. He, Y.L. Ge, G.W. Song, One-pot synthesis of boron and nitrogen co-doped carbon dots as the fluorescence probe for dopamine based on the redox reaction between Cr(VI) and dopamine, Sensor. Actuator. B Chem. 240 (2017) 1265–1271.
[10] Y. Xiong, J. Schneider, C.J. Reckmeier, H. Huang, P. Kasák, A.L. Rogach, Carbonization conditions influence the emission characteristics and the stability against photobleaching of nitrogen doped carbon dots, Nanoscale 9 (2017) 11730–11738.
[11] X. Miao, X.L. Yan, D. Qu, D.B. Li, F.F. Tao, Z.C. Sun, Red emissive sulfur, nitrogen codoped carbon dots and their application in ion detection and theraonostics, ACS Appl. Mater. Interfaces 9 (2017) 18549–18556.
[12] W.L. Gao, H.H. Song, X. Wang, X.Q. Liu, X.B. Pang, Y.M. Zhou, B. Gao, X.J. Peng, Carbon dots with red emission for sensing of Pt^{2+}, Au^{3+}, and Pd^{2+} and their bioapplications in vitro and in vivo, ACS Appl. Mater. Interfaces 10 (2018) 1147–1154.
[13] Y.H. Liu, W.X. Duan, W. Song, J.J. Liu, C.L. Ren, J. Wu, D. Liu, H.L. Chen, Red emission B, N, S-co-doped carbon dots for colorimetric and fluorescent dual mode detection of Fe^{3+} ions in complex biological fluids and living cells, ACS Appl. Mater. Interfaces 9 (2017) 12663–12672.
[14] Z.B. Guo, Y.F. Zheng, H. Xu, B.D. Zheng, W.W. Qiu, G.D. Liu, Lateral flow test for visual detection of silver(I) based on cytosine-Ag(I)-cytosine interaction in C-rich oligonucleotides, Microchim. Acta 184 (2017) 4243–4250.
[15] Y.R. Tang, H.J. Song, Y.Y. Su, Y. Lv, Turn-on persistent luminescence probe based on graphitic carbon nitride for imaging detection of biothiols in biological fluids, Anal. Chem. 85 (2013) 11876–11884.
[16] J. Zong, X.L. Yang, A. Trinchi, S. Hardin, I. Cole, Y.H. Zhu, C.Z. Li, T. Muster, G. Wei, Carbon dots as fluorescent probes for "off–on" detection of Cu^{2+} and L-cysteine in aqueous solution, Biosens. Bioelectron. 51 (2014) 330–335.
[17] Z. Li, Y. Wang, Y.N. Ni, S. Kokot, A rapid and label-free dual detection of Hg (II) and cysteine with the use of fluorescence switching of graphene quantum dots, Sens. Actuators B Chem. 207 (2015) 490–497.
[18] L. Zhou, Y.H. Lin, Z.Z. Huang, J.S. Ren, X.G. Qu, Carbon nanodots as fluorescence probes for rapid, sensitive, and label-free detection of Hg^{2+} and biothiols in complex matrices, Chem. Commun. (J. Chem. Soc. Sect. D) 48 (2012) 1147–1149.
[19] S. Liao, X.Y. Zhao, F.W. Zhu, M. Chen, Z.L. Wu, X.Z. Song, H. Yang, X.Q. Chen, S. Novel, N-doped carbon quantum dot-based "off-on" fluorescent sensor for silver ion and cysteine, Talanta 180 (2018) 300–308.
[20] V.K. Poon, A. Burd, In vitro cytotoxity of silver: implication for clinical wound care, Burns 30 (2004) 140–147.
[21] P.L. Drake, K.J. Hazelwood, Exposure-related health effects of silver and silver compounds: a review, Ann. Occup. Hyg. 49 (2005) 575–585.
[22] S.V. Mulay, Y. Kim, M. Choi, D.Y. Lee, J. Choi, Y. Lee, S. Jon, D.G. Churchill, Enhanced doubly activated dual emission fluorescent probes for selective imaging of glutathione or cysteine in living systems, Anal. Chem. 90 (2018) 2648–2654.
[23] H.F. Zhou, G.X. Ran, J.F. Masson, C. Wang, Y. Zhao, Q.J. Song, Rational design of magnetic micronanoelectrodes for recognition and ultrasensitive quantification of cysteine enantiomers, Anal. Chem. 90 (2018) 3374–3381.
[24] M. Chamsaz, M.H. Arbab-Zavar, J. Akhondzadeh, Triple-phase single-drop microextraction of silver and its determination using graphite-furnace atomic-absorption spectrometry, J. Anal. Sci. 24 (2008) 799–801.
[25] R. Mikelova, J. Baloun, J. Petrlova, V. Adam, L. Havel, J. Petrek, A. Horna, R. Kizek, Electrochemical determination of Ag-ions in environment waters and their action on plant embryos, Bioelectrochemistry 70 (2007) 508–518.
[26] W.B. Zhang, P.L. Li, Q.Q. Geng, Y.H. Duan, M.C. Guo, Y.S. Cao, Simultaneous determination of glutathione, cysteine, homocysteine, and cysteinylglycine in biological fluids by ion-pairing high-performance liquid chromatography coupled with precolumn derivatization, J. Agric. Food Chem. 62 (2014) 5845–5852.
[27] A. Küster, I. Tea, S. Sweeten, J. Rozé, R.J. Robins, D. Darmaun, Simultaneous determination of glutathione and cysteine concentrations and 2H enrichments in microvolumes of neonatal blood using gas chromatography-mass spectrometry, Anal. Bioanal. Chem. 390 (2008) 1403–1412.
[28] H. Huang, Y.H. Weng, L.H. Zheng, B.X. Yao, W. Weng, X.C. Lin, Nitrogen-doped carbon quantum dots as fluorescent probe for "off-on" detection of mercury ions, L-cysteine and iodide ions, J. Colloid Interface Sci. 506 (2017) 373–378.
[29] S. Huang, L.M. Wang, C.S. Huang, B.Q. Hu, W. Su, Q. Xiao, Graphene quantum dot coupled with gold nanoparticle based "off-on" fluorescent probe for sensitive and selective detection of L-cysteine, Microchim. Acta 183 (2016) 1855–1864.
[30] J. Feng, Y.Y. Ju, J.J. Liu, H.G. Zhang, X.G. Chen, Polyethyleneimine-templated copper nanoclusters via ascorbic acid reduction approach as ferric ion sensor, Anal. Chim. Acta 854 (2015) 153–160.
[31] S.Y. Yang, C.F. Wang, S. Chen, Interface-directed assembly of one-dimensional ordered architecture from quantum dots guest and polymer host, J. Am. Chem. Soc. 133 (2011) 8412–8415.
[32] K. Jiang, S. Sun, L. Zhang, Y.H. Wang, C.Z. Cai, H.W. Lin, Bright-yellow-emissive N-doped carbon dots: preparation, cellular imaging, and bifunctional sensing, ACS Appl. Mater. Interfaces 7 (2015) 23231–23238.
[33] Y.Q. Dong, H.C. Pang, H.B. Yang, C.X. Guo, J.W. Shao, Y.W. Chi, C.M. Li, T. Yu, Carbon-based dots co-doped with nitrogen and sulfur for high quantum yield and excitation-independent emission, Angew. Chem. Int 52 (2013) 1–6.
[34] S.Y. Zou, C.J. Hou, H.B. Fa, L. Zhang, Y. Ma, L. Dong, D. Li, D.Q. Huo, M. Yang, An efficient fluorescent probe for fluazinam using N, S co-dopedcarbon dots from L-cysteine, Sensor. Actuator. B Chem. 239 (2017) 1033–1041.
[35] X.W. Dong, Y.J. Su, H.J. Geng, Z.L. Li, C. Yang, X.L. Li, Y.F. Zhang, Fast one-step synthesis of N-doped carbon dots by pyrolyzing ethanolamine, J. Mater. Chem. C 2 (2014) 7477–7481.
[36] S. Sun, L. Zhang, K. Jiang, A.G. Wu, H.W. Lin, Toward high-efficient red emissive carbon dots: facile preparation, unique properties, and applications as

Please cite this article in press as: S. Huang, et al., Red emission nitrogen, boron, sulfur co-doped carbon dots for "on-off-on" fluorescent mode detection of Ag^+ ions and L-cysteine in complex biological fluids and living cells, Analytica Chimica Acta (2018), https://doi.org/10.1016/j.aca.2018.06.051

multifunctional theranostic agents, Chem. Mater. 28 (2016) 8659–8668.
[37] J.H. Liu, J.Z. Li, L.Q. Xu, Y.J. Qiao, J.C. Chen, Facile synthesis of N, B-doped carbon dots and their application for multisensor and cellular imaging, Ind. Eng. Chem. Res. 56 (2017) 3905–3912.
[38] Q. Wang, S.R. Zhang, Y.G. Zhong, X.F. Yang, Z. Li, H. Li, Preparation of yellow-green-emissive carbon dots and their application in constructing a fluorescent turn-on nanoprobe for imaging of selenol in living cells, Anal. Chem. 89 (2017) 1734–1741.
[39] P.F. Shen, Y.S. Xia, Synthesis-modification integration: one-step fabrication of boronic acid functionalized carbon dots for fluorescent blood sugar sensing, Anal. Chem. 86 (2014) 5323–5329.
[40] J. Schneider, C.J. Reckmeier, Y. Xiong, M. von Seckendorff, A.S. Susha, P. Kasák, A.L. Rogach, Molecular fluorescence in citric acid-based carbon dots, J. Phys. Chem. C 121 (2017) 2014–2022.
[41] J. Chen, J.S. Wei, P. Zhang, X.Q. Niu, W. Zhao, Z.Y. Zhu, H. Ding, H.M. Xiong, Red-emissive carbon dots for fingerprints detection by spray method: coffee ring effect and unquenched fluorescence in drying process, ACS Appl. Mater. Interfaces 9 (2017) 18429–18433.
[42] H.Y. Wang, Q.J. Lu, Y.X. Hou, Y.L. Liu, Y.Y. Zhang, High fluorescence S, N co-doped carbon dots as an ultra-sensitive fluorescent probe for the determination of uric acid, Talanta 155 (2016) 62–69.
[43] Y. Wang, S.H. Kim, L. Feng, Highly luminescent N, S- Co-doped carbon dots and their direct use as mercury(II) sensor, Anal. Chim. Acta 890 (2015) 134–142.
[44] Y.W. Zeng, D.K. Ma, W. Wang, J.J. Chen, L. Zhou, Y.Z. Zheng, K. Yu, S.M. Huang, N, S co-doped carbon dots with orange luminescence synthesized through polymerization and carbonization reaction of amino acids, Appl. Surf. Sci. 342 (2015) 136–143.
[45] Z.J. Li, Q.Y. Zhang, J.M. Pan, Recent advances with regard to triazene derivatives as chromogenic reagents in analytical chemistry, Rev. Anal. Chem. 22 (2003) 191–232.
[46] Y. Yoshida, Y. Ohiwa, M. Shimamura, T. Izumi, S. Yoshida, K. Takahashi, S. Miyairi, M. Makimura, A. Naganuma, Optimum conditions for derivatization of glutathione, cysteine and cysteinylglycine in human plasma with ammonium 7-fluorobenzo-2-oxa-1,3-diazole-4-sulfonate for accurate quantitation by high-performance liquid chromatography, J. Health Sci. 49 (2003) 527–530.

Please cite this article in press as: S. Huang, et al., Red emission nitrogen, boron, sulfur co-doped carbon dots for “on-off-on” fluorescent mode detection of Ag^{+} ions and L-cysteine in complex biological fluids and living cells, Analytica Chimica Acta (2018), https://doi.org/10.1016/j.aca.2018.06.051